ELSEVIER

SCIENCE DIRECT

PHYSICS LETTERS B

Physics Letters B 581 (2004) 263–269

www.elsevier.com/locate/physletb

Subleading critical exponents from the renormalisation group

Daniel F. Litim [a], Lautaro Vergara [b]

[a] *Theory Division, CERN, CH-1211 Geneva 23, Switzerland*
[b] *Departamento de Física, Universidad de Santiago de Chile, Casilla 307, Santiago 2, Chile*

Received 15 October 2003; accepted 18 November 2003

Editor: L. Alvarez-Gaumé

Abstract

We study exact renormalisation group equations for the 3d Ising universality class. At the Wilson–Fisher fixed point, symmetric and antisymmetric correction-to-scaling exponents are computed with high accuracy for an optimised cutoff to leading order in the derivative expansion. Further results are derived for other cutoffs including smooth, sharp and background field cutoffs. An estimate for higher order corrections is given as well. We establish that the leading antisymmetric corrections to scaling are strongly subleading compared to the leading symmetric ones.

PACS: 05.10.Cc; 05.70.Jk; 11.10.Hi

1. Introduction

Many physical systems with short range interactions and a scalar order parameter display Ising universal behaviour close to the critical point. Initially introduced for the study of magnetic systems, the Ising model also describes the physics of the liquid–gas phase transition, transitions in binary mixtures and in Coulombic systems [1]. In high energy physics, Ising universal behaviour is expected in various theories including the QCD phase transition with finite quark masses [2], the chiral phase transition of QCD [2,3], and the electro-weak phase transition [4].

The original Ising model has a global Z_2 symmetry. However, many systems in the Ising universality class like the liquid–gas and the electro-weak phase transition do not possess the Z_2 symmetry away from the critical point. The presence of operators odd under Z_2 lead to additional corrections-to-scaling exponents. In principle, deviations from Z_2 symmetric scaling are detectable experimentally. Antisymmetric corrections to scaling $\sim L^{-0.5}$ have been revealed in a Monte Carlo simulation of the electro-weak phase transition [4]. Previous theoretical studies of antisymmetric corrections to scaling are based on the ϵ-expansion [5], the scaling field method [6], and the Wegner–Houghton equation [7].

In this Letter, we study corrections to scaling for the 3d Ising universality class using the exact renormalisation group, which is based on the Wilsonian idea of successively integrating out momentum modes (see

E-mail addresses: daniel.litim@cern.ch (D.F. Litim), lvergara@lauca.usach.cl (L. Vergara).

0370-2693
doi:10.1016/j.physletb.2003.11.047

[8] for reviews and references therein). This approach is implemented through an infra-red cutoff which, within a few constraints, can be chosen freely. The strengths of the method are its flexibility and its numerical stability. Furthermore, a general optimisation procedure is available, enabling a choice of the infra-red cutoff best suited for the problem at hand [9]. To leading order in a derivative expansion, we employ an optimised cutoff and compute the first six subleading corrections-to-scaling exponents with high accuracy. We also obtain results for smooth, sharp and background field cutoffs, and estimate higher order corrections.

2. Renormalisation group and critical exponents

Renormalisation group methods have been used very successfully in the computation of universal observables at second order phase transitions. A particularly useful approach is the exact renormalisation group (ERG), based on the Wilsonian idea of integrating out momentum modes within a path integral representation of quantum field theory [8]. In its modern form, the ERG flow for an effective action Γ_k for bosonic fields φ is given by the simple one-loop expression

$$\partial_t \Gamma_k[\varphi] = \frac{1}{2}\,\mathrm{Tr}\big(\Gamma_k^{(2)} + R\big)^{-1}\partial_t R. \tag{1}$$

Here, $t \equiv \ln k$ is the logarithmic scale parameter, the trace denotes a momentum trace and a sum over indices, $\Gamma^{(2)}[\varphi](p,q) \equiv \delta^2\Gamma/\delta\varphi(p)\delta\varphi(q)$, and R is an infra-red momentum cutoff at the momentum scale k. The flow (1) interpolates between an initial (microscopic) action in the ultra-violet and the full quantum effective action in the infra-red. At every momentum scale k, (1) receives its main contributions for momenta about $p^2 \approx k^2$. The regulator can be chosen freely and allows for an optimisation of the flow within general approximations [9]. The optimisation entails improved convergence and stability properties of the flow. In combination with the numerical stability of the flow, it provides the basis for reliable predictions based on systematic approximations to (1). An important nonperturbative approximation scheme is the derivative expansion [10]. To leading order, the local potential approximation consists in the ansatz

$$\Gamma_k = \int d^dx \left(U_k(\varphi) + \frac{1}{2}\partial_\mu\varphi\partial_\mu\varphi \right) \tag{2}$$

for the effective action. It implies that higher order corrections proportional to the anomalous dimension η of the fields are neglected. For the Ising universality class, η is of the order of a few percent. Inserting the ansatz (2) into the flow equation (1) and evaluating it for constant fields leads to the flow for the effective potential U_k. We introduce dimensionless variables $u(\phi) = U_k/k^d$ and $\phi = \varphi k^{1-d/2}$. Then, finding a fixed point amounts to solving $\partial_t u = 0$. To that end we employ a polynomial truncation of the fixed point potential, retaining vertex functions ϕ^n up to a maximum number n_{trunc},

$$u(\phi) = \sum_{n=1}^{n_{\mathrm{trunc}}} \frac{1}{n!}\tau_n\phi^n. \tag{3}$$

The potential has been normalised as $u(\phi = 0) = 0$. The ansatz (3) leads to n_{trunc} ordinary differential equations $\partial_t\tau_i \equiv \beta_i$. In three Euclidean dimensions, the flow equation exhibits the nontrivial Wilson–Fisher fixed point $u_* \neq 0$. Universal critical exponents and corrections-to-scaling exponents are obtained as the eigenvalues of the stability matrix at criticality $M_{ij} = \partial\beta_i/\partial\tau_j|_*$. For convenience, we introduce the set of ϕ-even couplings $\lambda_n = \tau_{2n}$ and ϕ-odd couplings $\bar\lambda_n = \tau_{2n-1}$. Under reflection in field space the couplings and their β-functions behave as

$$\phi \to -\phi\text{:}\quad \begin{cases} (\lambda, \bar\lambda) \to (\lambda, -\bar\lambda), \\ (\beta_\lambda, \beta_{\bar\lambda}) \to (\beta_\lambda, -\beta_{\bar\lambda}). \end{cases} \tag{4}$$

The scaling solution is symmetric under $\phi \to -\phi$. Hence all ϕ-odd couplings $\bar\lambda_*$ vanish at the fixed point. The computation of critical exponents is simplified by observing that $\beta_{\bar\lambda}(\lambda,\bar\lambda) = -\beta_{\bar\lambda}(\lambda,-\bar\lambda)$ for all λ. This follows from (3) and (4). In particular, $\beta_{\bar\lambda}$ vanishes identically at $\bar\lambda = 0$, where all derivatives of $\beta_{\bar\lambda}$ w.r.t. the symmetric couplings vanish at the fixed point. Therefore, the stability matrix M at criticality simplifies and becomes equivalent to the matrix

$$\begin{pmatrix} A & B \\ 0 & C \end{pmatrix} \tag{5}$$

with $A \equiv \partial\beta_\lambda/\partial\lambda|_*$, $B \equiv \partial\beta_\lambda/\partial\bar\lambda|_*$ and $C \equiv \partial\beta_{\bar\lambda}/\partial\bar\lambda|_*$. In consequence, the eigenvalues of M reduce to those

of the submatrices A and C. The matrix A carries the information about the critical exponent ν and the symmetric corrections to scaling, while the matrix C contains the information about antisymmetric corrections to scaling.

3. Results

In this section, we present our results for the universal eigenvalues of the stability matrix. The fixed point is determined in truncations up to $n_{\rm trunc} = 40$. The optimised regulator $R_{\rm opt} = (k^2 - q^2)\theta(k^2 - q^2)$ is employed to improve the convergence and stability of the flow [9,11,12]. The stability matrix is evaluated with two different methods: an expansion in powers of the field about vanishing field, and an expansion in Legendre polynomials. The latter case involves an integration in field space.

Our numerical results are given in Tables 1 and 2, and in Figs. 1–4. First, we discuss our results for the ϕ-even corrections to scaling. In Fig. 1, the three leading eigenvalues of A are displayed, ν^{-1}, ω and ω_2. Notice that the eigenvalues are identical for truncations $(n, n+1)$, if n is even. The reason for this is simple: increasing the truncation by a ϕ-odd coupling does neither change the dimension of the matrix A, nor the numerical values of the fixed couplings (because ϕ-odd couplings vanish at the fixed point). Hence, the ϕ-even eigenvalues remain unchanged, as is clearly seen in Fig. 1. The numerical values for the ϕ-even eigenvalues are identical to those which are found in a polynomial expansion in $\rho = \phi^2/2$.

Next, we turn to the ϕ-odd corrections to scaling (Figs. 2–4). We have computed the eigenvalues of the

Table 1
ϕ-even and ϕ-odd eigenvalues ($R_{\rm opt}$, $n_{\rm trunc} = 40$)

ϕ-even		ϕ-odd	
		y_h	-2.5
ν	0.6495	$y_{\rm shift}$	-0.5
ω_1	0.655	$\bar{\omega}_1$	1.88
ω_2	3.18	$\bar{\omega}_2$	4.5
ω_3	5.9	$\bar{\omega}_3$	7

Table 2
ϕ-even and ϕ-odd eigenvalues ($R_{\rm opt}$, $n_{\rm trunc} = 22$, $\phi_{\rm max} = 0.46$)

ϕ-even		ϕ-odd	
		y_h	-2.5
ν	0.649562	$y_{\rm shift}$	-0.5
ω_1	0.6557	$\bar{\omega}_1$	1.886
ω_2	3.180	$\bar{\omega}_2$	4.524
ω_3	5.912	$\bar{\omega}_3$	7.33

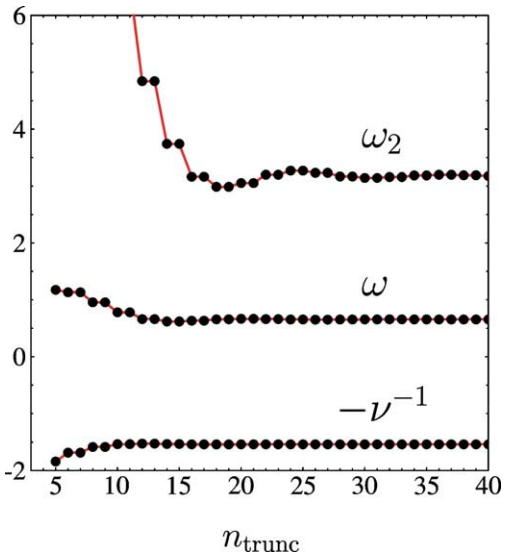

Fig. 1. The exponents ν, ω and ω_2 from a polynomial truncation to order $n_{\rm trunc}$ about vanishing field.

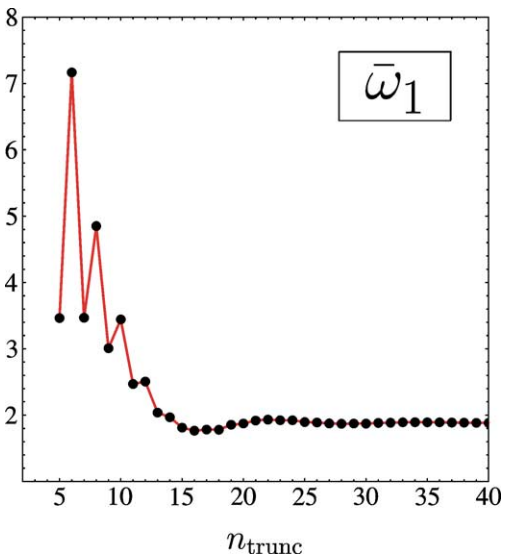

Fig. 2. The exponent $\bar{\omega}_1$ (see Fig. 1).

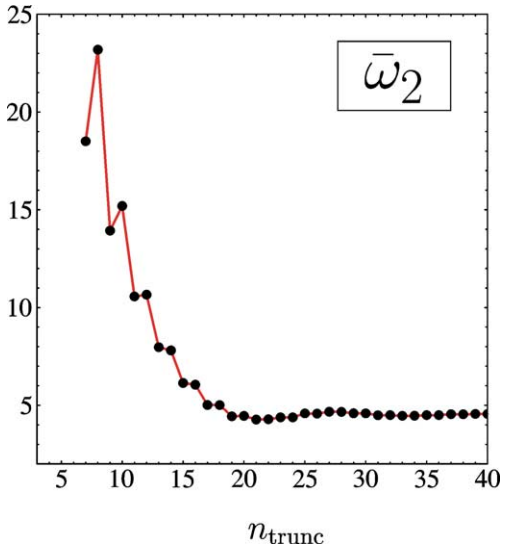

Fig. 3. The exponent $\bar{\omega}_2$ (see Fig. 1).

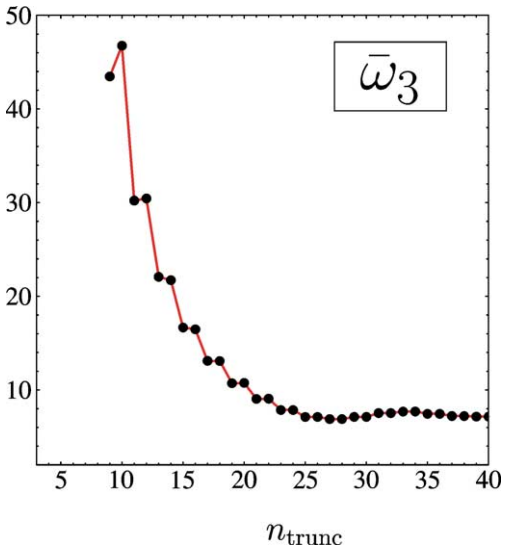

Fig. 4. The exponent $\bar{\omega}_3$ (see Fig. 1).

matrix C for $n_{\rm trunc}$ up to $n_{\rm trunc} = 40$. We find two eigenvalues $y_h = -5/2$ and $y_{\rm shift} = -1/2$, related to redundant operators [6]. All other eigenvalues are positive. We denote them as $\bar{\omega}_n$. The leading non-trivial ϕ-odd correction-to-scaling exponent $\bar{\omega}_1$ as a function of the truncation is displayed in Fig. 2. (In the literature, $\bar{\omega}_1$ is sometimes denoted as ω_A or ω_5.) Our results for $\bar{\omega}_2$ and $\bar{\omega}_3$ are given in Figs. 3 and 4, respectively. Notice that the pattern of the results, with increasing truncation, is similar to the pattern found in the ϕ-even sector. The results for two subsequent truncations $(n, n+1)$ for n odd are close to each other for sufficiently large truncation. The reason for this is the following: increasing the truncation by a ϕ-even coupling does not change the dimension of the matrix C. However, it does change the numerical value of the fixed point, and hence the eigenvalues of C. With increasing truncation, the numerical change within the ϕ-even couplings at the fixed point is very small and eventually, the eigenvalues of C become insensitive to the addition of a ϕ-even coupling. This is nicely observed in the results presented in Figs. 2–4. Comparing the symmetric with the antisymmetric corrections to scaling, the general pattern we find is that $0 < \omega_1 < \bar{\omega}_1 < \cdots < \omega_n < \bar{\omega}_n < \cdots$.

We have also computed the critical exponents by using the approach of [7]. Expanding the scaling potential and the eigenperturbations in terms of orthogonal polynomials (Legendre polynomials) implies that the matrix elements of (5) involve an integration in field space $\phi \in [-\phi_{\rm max}, \phi_{\rm max}]$. The weak dependence on $\phi_{\rm max}$ is fixed by requiring that the ϕ-even eigenvalues agree to high accuracy with the known values obtained in [12] using an expansion in $\rho = \phi^2/2$ about the potential minimum $\rho = \rho_0$. This procedure improves the numerical convergence. Our results for the eigenvalues are given in Table 2. They are consistent with and have a higher accuracy than those given in Table 1.

Next we discuss our results based on other regularisations including the power law cutoff, the sharp cutoff and a background field cutoff. Varying the momentum dependence of the regulator R from "smooth" to "sharp" allows for an estimate of higher order corrections due to operators neglected in the present approximation, e.g., [13]. We have computed the ϕ-even and ϕ-odd eigenvalues for a smooth power-like regulator $R_{\rm quartic} = k^2 \cdot (q^4/k^4)$, for the sharp cutoff $R_{\rm sharp} = \lim_{a\to\infty} ak^2\theta(k^2-q^2)$, and for a background field cutoff $R_{\rm bg}$. Results are summarised in Fig. 5 and Table 3.

The power-law cutoff $R_{\rm quartic}$ is optimised in the sense of [9]. We find that the flow based on $R_{\rm quartic}$ has similar stability and convergence properties as the flow with $R_{\rm opt}$, e.g., Fig. 5. Also, the numerical results as given in Table 3 are within 5% or less

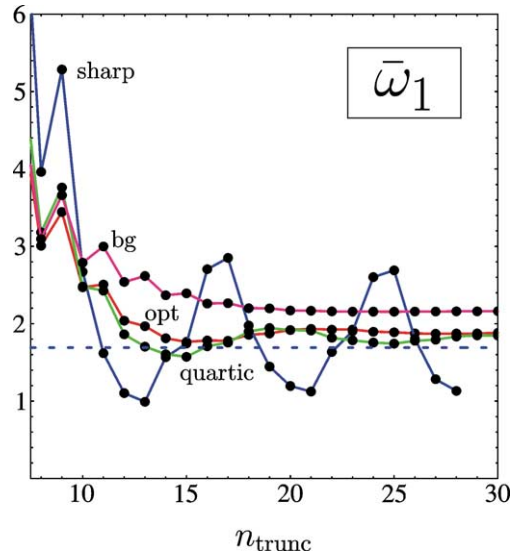

Fig. 5. The exponent $\bar{\omega}_1$ from a polynomial expansion up to order $n_{\rm trunc}$, and in comparison for the sharp, the background field (bg), the optimised (opt) and the quartic cutoff (see text).

to each other. The sharp cutoff does not lead to an optimised flow [9]. It displays instabilities within a local polynomial expansion about vanishing field [12, 14]. This is confirmed in our analysis. In Fig. 5, the ϕ-odd eigenvalue $\bar{\omega}_1$ is displayed up to a truncation $n_{\rm trunc} = 30$. The local field expansion based on $R_{\rm sharp}$ oscillates in the eight-fold pattern $(++++----)$ about its mean value, reminiscent of the four-fold pattern in an expansion in ϕ^2 [12]. The expansion fails to converge at the present order. The asymptotic value for $\bar{\omega}_1$ is indicated by the dashed line. Moreover, the eigenvalues for $n_{\rm trunc} = 16, 17, 24$ and 25 possess a small imaginary part, which is not displayed in Fig. 5. These findings are a reflection of an intrinsic instability of the sharp cutoff flow. Furthermore, the sharp cutoff value for the leading critical exponent ν is $\sim 8\%$ larger than the value for $R_{\rm opt}$ [11], and $\sim 10\%$ larger than the physical value. These properties indicate that quantitative results from the sharp cutoff flow within a given truncation, although qualitatively correct, are less reliable than those by optimised cutoffs.

The instability in the stability matrix of the sharp cutoff flow is removed by expanding the fixed point potential and the eigenperturbations in terms of Legendre polynomials. For the eigenvalues, we adjust $\phi_{\rm max}$ as described above to improve the numerical convergence. Our results are given in Table 3, and by the dashed line in Fig. 5. In the ϕ-even sector, our results agree to all significant digits with those by Morris (quartic cutoff) [15], Comellas and Travesset (sharp cutoff) [16] and Litim (optimised cutoff) [12]. This provides a nontrivial consistency check, because the numerical methods employed in [15,16], in [12], and here, are all different. The main new results concern the eigenvalues in the ϕ-odd sector, where we also confirm the first two eigenvalues by Tsypin (sharp cutoff) [7] (see also [17]).

Now we proceed with the background field flow, where plain momenta q^2 in the regulator are replaced by $\Gamma^{(2)}[\bar{\phi}]$, the full inverse propagator evaluated at some background field $\bar{\phi}$ [18] (see also [19]). Identifying the background field with the physical mean leads to a partial diagonalisation, which should further stabilise the flow. Background field flows are closely related to the proper-time renormalisation group of Liao [20], to which they reduce once an additional flow term proportional to $\partial_t \Gamma^{(2)}$ is dropped. Implicit to this approach is that differences between fluctuation and background field are neglected—an approximation, which in the present theory becomes exact in the infra-red limit. Hence, as detailed in [18], we expect this approximation to be viable in the vicinity of a critical point.

Table 3
ϕ-even and ϕ-odd eigenvalues for the sharp, quartic, optimised and background field cutoff, using $\phi_{\rm max} = 0.43, 0.45, 0.46$, and 0.46, respectively (see text)

ϕ-even	$R_{\rm sharp}$	$R_{\rm quartic}$	$R_{\rm opt}$	$R_{\rm bg}$	ϕ-odd	$R_{\rm sharp}$	$R_{\rm quartic}$	$R_{\rm opt}$	$R_{\rm bg}$
ν	0.6895	0.6604	0.649562	0.625979					
ω_1	0.5952	0.6285	0.6557	0.762204	$\bar{\omega}_1$	1.691	1.812	1.886	2.163
ω_2	2.838	3.048	3.180	3.6845	$\bar{\omega}_2$	3.998	4.32	4.524	5.313
ω_3	5.18	5.63	5.912	7.038	$\bar{\omega}_3$	6.38	6.96	7.33	8.85

Here, we use the flow $\partial_t \Gamma_k = \mathrm{Tr} \exp -\Gamma_k^{(2)}/k^2$ to leading order in a derivative expansion. It is a background field flow in the proper-time approximation with regulator $R_{\rm bg}$ given by (13), (14) of [18]. Amongst the proper-time flows, it has best stability properties [21] (see also [11]). This is reflected by the very fast convergence of $\bar{\omega}_1$ with the truncation (Fig. 1). We also stress that the first two eigenvalues in the ϕ-even sector, which agree with earlier results in [21,22], are very close to the physical values. The further subleading corrections-to-scaling exponents are increasingly larger than the values for $R_{\rm opt}$. This trend is indicative for the potential effect of higher order corrections.

Finally we comment on the Polchinski renormalisation group [23]. It is related to the flow (1) by a Legendre transform and additional field rescalings. In consequence, both methods have inequivalent derivative expansions. To leading order, the Polchinski flow is independent of the regularisation [24], in contradistinction to the present approach, e.g., [12]. For $R_{\rm opt}$, critical exponents in the ϕ-even sector agree to high precision with those from the Polchinski flow. The numerical value for the ϕ-odd eigenvalue $\bar{\omega}_1$ given in Table 2 for $R_{\rm opt}$, also agrees with preliminary results from the Polchinski flow [25]. If these findings persist, they confirm the deeper link between the two methods even for the ϕ-odd sector.

4. Discussion and conclusion

We have studied symmetric and antisymmetric corrections to scaling at criticality for systems belonging to the 3d Ising universality class. The first six subleading universal corrections-to-scaling exponents are obtained from an exact renormalisation group. Best results are achieved for optimised flows, which have enhanced convergence and stability properties. In addition, we have assessed the cutoff dependence for smooth, sharp and a background field cutoff. This study also served as an indicator for higher order effects. Results from the standard and the background field flows have to be seen on slightly different footings due to qualitative differences in the approximations.

For the optimised flow, the leading symmetric and antisymmetric correction-to-scaling exponents are $\omega = 0.6557$ and $\omega_A = 1.886$. For different regularisations ranging from sharp to optimised cutoffs and including (excluding) the background field flow, the exponents vary between $\omega \approx 0.60$–0.76 (0.60–0.66) and $\omega_A \approx 1.7$–2.2 (1.7–1.9). Higher order corrections due to a nonvanishing anomalous dimension lead to $\omega \approx 0.8$, and similar corrections are expected for ω_A. Expressed in terms of the exponent $\Delta_A = \omega_A \nu$, our results are $\Delta_A \approx 1.22$ for the optimised, $\Delta_A \approx 1.2$ for the quartic, $\Delta_A \approx 1.17$ for the sharp and $\Delta_A \approx 1.35$ for the background field cutoff. This compares well with $\Delta_A \approx 1.3$ which is often assumed in the analysis of experimental data, e.g., [26]. The leading symmetric corrections to scaling are $\Delta = \omega\nu \approx 0.42$–$0.48$, increasing towards $\Delta \approx 0.52$ once anomalous dimensions are taken into account. This cutoff dependence indicates the expected size of higher order effects. Our results for ω_A are consistent with the estimate $\omega_A > 1.5$ based on Padé resummation of the ϵ-expansion [5], and with $\omega_A \approx 2.4$ from the scaling field method [6]. We notice that all sharp cutoff eigenvalues are systematically smaller than those from any other cutoff. This reflects, we believe, the notoriously poor convergence behaviour of sharp cutoff flows.

In conclusion, we have established that the leading antisymmetric corrections to scaling are consistently suppressed compared to the leading symmetric ones. Within the errors, the exponent ω_A is more than twice as big as ω. Hence, the scaling behaviour $\sim L^{-0.5}$ as seen in a Monte Carlo simulation of the electro-weak theory clearly dominates over both the leading symmetric $\sim L^{-\omega}$ and antisymmetric $\sim L^{-\omega_A}$ corrections to scaling and therefore cannot be explained with the exponent ω_A.

Acknowledgements

L.V. would like to thank C. Bervillier for e-mail correspondence. D.F.L. thanks the University of Santiago de Chile for hospitality. This work was supported in part by Fondecyt-CHILE Nos. 1020061 and 7020061.

References

[1] A. Pelissetto, E. Vicari, Phys. Rep. 368 (2002) 549, cond-mat/0012164.
[2] R.D. Pisarski, F. Wilczek, Phys. Rev. D 29 (1984) 338.
[3] S. Gavin, A. Gocksch, R.D. Pisarski, Phys. Rev. D 49 (1994) 3079, hep-ph/9311350;
F. Karsch, E. Laermann, C. Schmidt, Phys. Lett. B 520 (2001) 41, hep-lat/0107020.
[4] K. Rummukainen, M. Tsypin, K. Kajantie, M. Laine, M.E. Shaposhnikov, Nucl. Phys. B 532 (1998) 283, hep-lat/9805013.
[5] F.J. Wegner, Phys. Rev. B 6 (1972) 1891;
J.F. Nicoll, Phys. Rev. A 24 (1981) 2203;
J.F. Nicoll, R.K.P. Zia, Phys. Rev. B 23 (1981) 6157;
F.C. Zhang, R.K.P. Zia, J. Phys. A 15 (1982) 3303.
[6] E.K. Newman, K.E. Riedel, Phys. Rev. B 30 (1984) 6615.
[7] M.M. Tsypin, Nucl. Phys. B 636 (2002) 601, hep-lat/0112001.
[8] C. Bagnuls, C. Bervillier, Phys. Rep. 348 (2001) 91, hep-th/0002034;
J. Berges, N. Tetradis, C. Wetterich, Phys. Rep. 363 (2002) 223, hep-ph/0005122;
J. Polonyi, Central Eur. Sci. J. Phys. 1 (2002) 1, hep-th/0110026.
[9] D.F. Litim, Phys. Lett. B 486 (2000) 92, hep-th/0005245;
D.F. Litim, Phys. Rev. D 64 (2001) 105007, hep-th/0103195;
D.F. Litim, Int. J. Mod. Phys. A 16 (2001) 2081, hep-th/0104221;
D.F. Litim, hep-th/0208117.
[10] G.R. Golner, Phys. Rev. B 33 (1986) 7863.
[11] D.F. Litim, JHEP 0111 (2001) 059, hep-th/0111159.
[12] D.F. Litim, Nucl. Phys. B 631 (2002) 128, hep-th/0203006.
[13] F. Freire, D.F. Litim, Phys. Rev. D 64 (2001) 045014, hep-ph/0002153.
[14] A. Margaritis, G. Odor, A. Patkos, Z. Phys. C 39 (1988) 109.
[15] T.R. Morris, Phys. Lett. B 329 (1994) 241, hep-ph/9403340.
[16] J. Comellas, A. Travesset, Nucl. Phys. B 498 (1997) 539, hep-th/9701028.
[17] C. Bagnuls, C. Bervillier, M. Shpot, unpublished.
[18] D.F. Litim, J.M. Pawlowski, Phys. Lett. B 546 (2002) 279, hep-th/0208216.
[19] D.F. Litim, J.M. Pawlowski, Phys. Rev. D 66 (2002) 025030, hep-th/0202188;
D.F. Litim, J.M. Pawlowski, Phys. Rev. D 65 (2002) 081701, hep-th/0111191.
[20] S.B. Liao, Phys. Rev. D 53 (1996) 2020, hep-th/9501124.
[21] D.F. Litim, J.M. Pawlowski, Phys. Lett. B 516 (2001) 197, hep-th/0107020.
[22] M. Mazza, D. Zappala, Phys. Rev. D 64 (2001) 105013, hep-th/0106230.
[23] J. Polchinski, Nucl. Phys. B 231 (1984) 269.
[24] R.D. Ball, P.E. Haagensen, J.I. Latorre, E. Moreno, Phys. Lett. B 347 (1995) 80.
[25] C. Bervillier, private communication.
[26] A. Kostrowicka Wyczalkowska, J.V. Sengers, J. Chem. Phys. 111 (1999) 1551.